

Quantitative Imaging of Perfusion Using a Single Subtraction (QUIPSS and QUIPSS II)

Eric C. Wong, Richard B. Buxton, Lawrence R. Frank

In the pulsed arterial spin labeling (ASL) techniques EPICSTAR, PICORE, and FAIR, subtraction of two images in which inflowing blood is first tagged and then not tagged yields a qualitative map of perfusion. An important reason this map is not quantitative is that there is a spatially varying delay in the transit of blood from the tagging region to the imaging slice that cannot be measured from a single subtraction. We introduce here two modifications of pulsed ASL (QUIPSS and QUIPSS II) that avoid this problem by applying additional saturation pulses to control the time duration of the tagged bolus, rendering the technique relatively insensitive to transit delays and improving the quantitation of perfusion.

Key words: QUIPSS; QUIPSS II; perfusion; cerebral blood flow.

INTRODUCTION

Quantitative noninvasive imaging of perfusion is a goal of several existing imaging techniques, including radio-tracer techniques such as positron emission tomography and single photon emission computed tomography and MRI-based arterial spin labeling (ASL) techniques. Potential applications of these techniques include evaluation of resting perfusion for diagnosis of vascular diseases such as stroke and functional mapping of the brain (1–3). In the MRI-based techniques, arterial blood is magnetically tagged by inversion, and the flow of tagged blood into the imaging slice is measured. Unlike radio-tracer techniques, injection of external agents is not required, higher spatial resolution is achievable, and coregistration with high-resolution anatomical MRI data is straightforward.

MRI methods can be subdivided into continuous ASL techniques, which continuously invert blood flowing into a slice (4, 5), and pulsed ASL techniques, which periodically invert a block of arterial blood and measure the arrival of that blood into the imaging slice. Examples of pulsed ASL techniques include EPICSTAR (6), PICORE (7, 8), and flow-sensitive inversion recovery. The latter was introduced by Kwong *et al.* (3) and later referred to as FAIR (9). For both continuous and pulsed ASL, an important source of systematic error in the quantitation of perfusion is the delay between the application of the tag and the arrival of tagged blood into the imaging slice. This delay creates a spatially variable amount of T_1 decay of the tagged blood upon arrival into the imaging slice (8,

10, 11) and can strongly affect the amount of tagged blood that has been delivered at the time of image acquisition. Because this delay in humans is on the same order as T_1 , it can significantly affect the calculated perfusion. Pulsed ASL techniques allow one to measure the spatial distribution of delay times and correct for them in perfusion calculations. In these techniques, a series of measurements are taken alternately with and without the inversion tag and for a series of different delay times (TIs) after the inversion tag. Pairwise subtraction of images with and without the inversion tag gives a perfusion-related signal. To calculate perfusion using these techniques, we use a kinetic model of tagged blood simultaneously flowing into the slice and decaying (7, 8), whereas others have modeled the inflow process as a perturbation of the apparent T_1 decay of the static tissue (4, 5, 9, 12). Because the delay time is not known *a priori*, a minimum of two subtractions at different TIs (four images) are required to estimate both the delay and the perfusion in each voxel. Although several studies have reported quantitative cerebral blood flow (CBF) values using pulsed ASL (9, 12, 13), in these, the transit delay is assumed to be zero.

We describe here two modifications of pulsed ASL that, in principle, allow for elimination of the effects of this variable transit delay using a single subtraction of two images and refer to these techniques as QUIPSS (QUantitative Imaging of Perfusion using a Single Subtraction) and QUIPSS II. We have previously reported preliminary data on these techniques in abstract form (10, 14).

THEORY

In pulsed ASL, arterial blood is tagged proximal to the imaging slice by inversion, and sequential images are acquired in which blood is alternately inverted and not inverted. We refer to these as tag and control states, respectively. Subtraction of tag from control images then leaves a difference signal ΔM that can be expressed as (8, 15, 16)

$$\Delta M(t) = \begin{cases} 0 & t < \delta t \\ 2M_{0B}f(t - \delta t)e^{-t/T_{1B}} q(T_{1B}, T_{1T}, T_{ex}, f, \lambda, t) & \delta t < t < \delta t + \tau \\ 2M_{0B}f\tau e^{-t/T_{1B}} q(T_{1B}, T_{1T}, T_{ex}, f, \lambda, t) & \delta t + \tau < t \end{cases} \quad [1]$$

where f is the CBF in (ml of blood)/(ml of tissue)/min, δt is the transit delay from the application of the tag to the first arrival of tagged blood in the imaging slice, τ is the time width of the tag, M_{0B} is the relaxed magnetization of arterial blood, T_{1B} and T_{1T} are the T_1 values of arterial

MRM 39:702–708 (1998)

From the Departments of Radiology (E.C.W., R.B.B., L.R.F.) and Psychiatry (E.C.W.), University of California San Diego, San Diego, California.

Address correspondence to: Dr. Eric C. Wong, Thornton Hospital Radiology 7756, La Jolla, CA 92037.

Received September 10, 1997; revised December 16, 1997; accepted January 14, 1998.

0740-3194/98 \$3.00

Copyright © 1998 by Williams & Wilkins

All rights of reproduction in any form reserved.

blood and brain parenchyma, respectively, T_{ex} is the time after application of the tag at which the tagged water exchanges into brain tissue, and λ is the brain:blood partition coefficient of water. It should be noted that the definition of perfusion used here is slightly different from the definition of perfusion as measured using radio-labeled microspheres. The MRI-based measurement naturally measures the volume of blood delivered to a volume of space per unit time, whereas microspheres measure the volume of blood delivered per unit weight of tissue per unit time.

The terms $f(t - \delta t)$ in the second line and $f\tau$ in the third line are simply the volume of blood that has entered a voxel. The exponential term accounts for the T_1 decay of the tagged blood, and the factor of 2 is present because the difference in magnetization between inverted and noninverted blood is $2M_{0B}$. The factor q is a correction term that accounts for two effects: a shift in the T_1 decay of the tag due to exchange of tagged magnetization from blood into brain tissue, and clearance of the tag by outflow. Both of these effects are relatively small, and in practice, q is close to unity (typically 0.85–1.0). These effects are discussed in more detail elsewhere (8, 15–17). The raw difference signal ΔM , although proportional to f , does not provide sufficient data to construct a perfusion map, primarily because δt and τ are not known. M_{0B} and T_{1B} are spatially invariant constants that can be estimated either from imaging measurements or assumed from literature values and simply scale the perfusion measurement. The parameters δt and τ are both dependent on vessel geometry and the distribution of flow velocities. We have previously estimated that in normal volunteers both are typically on the order of 700 ms for a 10-cm tag and a 1-cm gap from tag to imaging slice but that δt can vary across a single slice from approximately 400 ms to over 1200 ms (18, 19).

We describe here two modifications of the basic pulsed ASL experiment that are both aimed at eliminating the dependence of ΔM on δt and τ and, although they seem nearly identical in implementation, have very different properties.

QUIPSS (I)

In QUIPSS, a saturation pulse is applied to the imaging slice at time TI_1 after the application of the tag (Fig. 1). Because this pulse is applied for both the tag and control images, it effectively removes any contribution to the difference signal of blood that arrives before TI_1 . The image is acquired at time TI_2 , after a delay of $\Delta TI \equiv TI_2 - TI_1$ from the time of the saturation pulse. Thus, only tagged blood that enters the imaging slice between TI_1 and TI_2 contribute to the difference signal. If

$$\begin{aligned} TI_1 &> \delta t \\ TI_2 &< \delta t + \tau \end{aligned} \quad [2]$$

then tagged blood is entering the slice for the entire time ΔTI , and the difference signal is given by

$$\begin{aligned} \Delta M(TI_2) &= 2M_{0B}f\Delta TI e^{-TI_2/T_{1B}} \\ &\cdot q(T_{1B}, T_{1t}, T_{ex}, f, \lambda, TI_2). \end{aligned} \quad [3]$$

Under these circumstances, the terms δt and τ do not appear at all, having been replaced by the pulse sequence parameter ΔTI , greatly simplifying the calculation of f .

QUIPSS II

QUIPSS II is identical to QUIPSS, except that the saturation pulse is applied to the tagging region rather than the imaging slice (Fig. 1). In this case, the only tagged blood that contributes to the signal is that which leaves the tagging region in the time TI_1 after the tag, producing a tagged bolus of sharply defined time width TI_1 . If

$$\begin{aligned} TI_1 &< \tau \\ TI_2 &> TI_1 + \delta t \end{aligned} \quad [4]$$

then a tagged bolus of time duration TI_1 leaves the tagging region and enters the imaging slice before image acquisition. In this case, the difference signal is given by

$$\Delta M(TI_2) = 2M_{0B}fTI_1 e^{-TI_2/T_{1B}} q(T_{1B}, T_{1t}, T_{ex}, f, \lambda, TI_2). \quad [5]$$

Again, δt and τ do not appear, but the difference signal is now proportional to the pulse sequence parameter TI_1 .

Thus, if the conditions on TI_1 and TI_2 are met (Eqs. [2] and [4]), then the difference signal is independent of both δt and τ , and f can be calculated from a single subtraction. The non-QUIPSS alternative for quantitative measurement of perfusion is to acquire difference images at two or more values of TI and fit the data for both f and δt , according to Eq. [1]. For longer values of TI, τ must be estimated from the data as well.

Because M_{0B} and T_{1B} are spatially invariant and q is a small correction term, f dominates the spatial distribution of ΔM , and the subtracted image is itself a quantitative map of the relative perfusion across the slice. If M_{0B} and T_{1B} are known, then an absolute scale can be placed on the perfusion image.

METHODS

The pulse sequence for QUIPSS is shown in Fig. 2. In this study, PICORE (7, 8) tagging is used, although we have also used both EPSTAR and FAIR tagging with nearly identical results. In PICORE, the tag condition uses a slab-selective inversion proximal to the imaging slice, and the control condition uses the same RF pulse as the tag, but in the absence of gradients, and at the same resonance offset relative to the imaging slice as the tag. The inversion pulse is immediately preceded by an in-plane saturation pulse to improve the subtraction of static tissue between the two tagging conditions (6). This pulse minimizes the interaction between the slab-selective inversion tag and the static tissue in the imaging slice.

Imaging was performed on a GE SIGNA 1.5 T system (General Electric Medical Systems, Milwaukee, WI) fitted with local head gradient and RF coils of our own design (20–22). Single-shot blipped echo-planar imaging (EPI) was used at 64×64 resolution, with FOV = 24 cm, and slice thickness = 8 mm. For inversion, a 15-ms adiabatic hyperbolic secant pulse (23) was used with parameters $\mu = 10$ and $\beta = 800 \text{ s}^{-1}$. A 10-cm inversion was used for

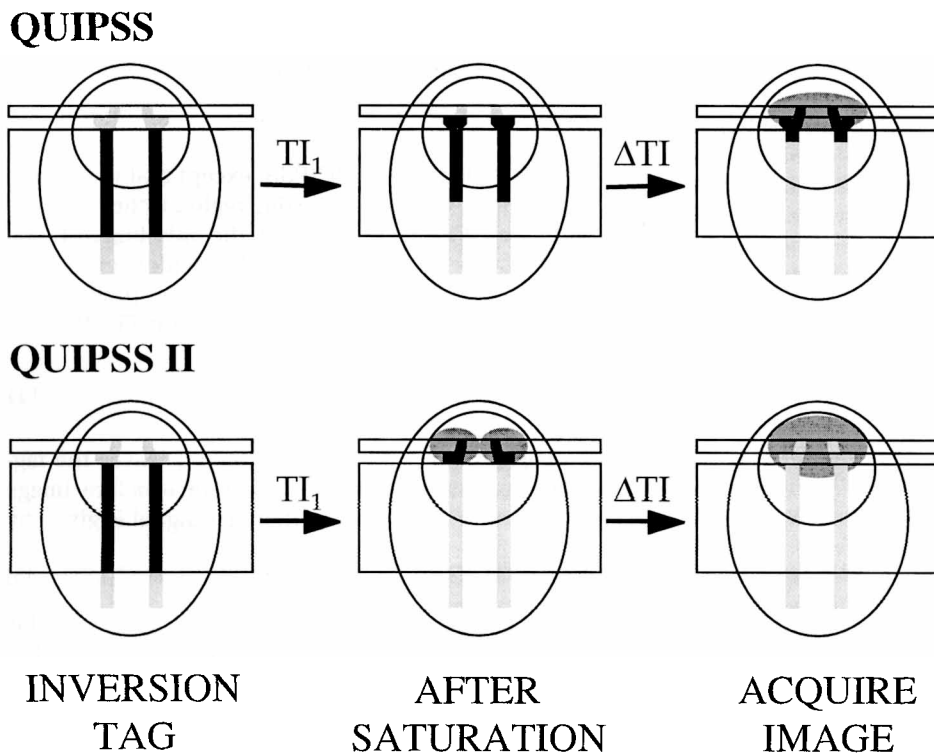


FIG. 1. Schematic representations of QUIPSS and QUIPSS II. Black represents blood that is inverted in the tag state but not in the control state, and gray represents tagged blood as it distributes into brain tissue. In both QUIPSS and QUIPSS II, a slab of blood proximal to the imaging plane is tagged (left column). In QUIPSS, the imaging plane is saturated at time T_{I1} , after which tagged blood immediately begins to enter the slice (middle column). If the conditions of Eq. [2] are met, then tagged blood continues to enter the slice until the image is acquired at time T_{I2} (right column). In QUIPSS II, the tagging region is saturated at time T_{I1} , ensuring that an amount of blood equal to $T_{I1}f$ has left the tagging region (middle column). If the tagged blood reaches the imaging slice (Eq. [4]) by time T_{I2} , then the difference image collected at time T_{I2} should be proportional to $T_{I1}f$ (right column).

the tag, leaving a 1-cm gap between the distal edge of the tagging region and the proximal edge of the imaging slice. This gap was found to be necessary to obtain good subtraction of static tissue (24), even in the presence of the in-plane presaturation pulse. Using direct integration of the Bloch equations, including relaxation and flow effects, we calculate that the inversion efficiency of this pulse is $>97\%$ for flow from 0–100 cm/s. Other imaging parameters were: TE = 25 ms for gradient-recalled EPI and 45 ms for spin-echo EPI; TR = 2000 ms; and T_{I1}/T_{I2} were typically 600 ms/1200 ms. One hundred images (50 tag-control pairs) were acquired and averaged for each perfusion map, for an imaging time of 3 min 20 s. The saturation at T_{I1} was performed using 90° Hanning windowed sinc pulses with 16 zero crossings. For more complete saturation, two such pulses were applied consecutively, separated, and followed by 4-ms spoiling gradients.

For multislice imaging, QUIPSS II was used, and multiple slice locations were imaged in rapid succession after one tag or control pulse. QUIPSS (I) is not amenable to multislice imaging because it requires saturation of the imaging slice without perturbation of more proximal tissues, and it is not possible to satisfy this condition for multiple slices. In QUIPSS II, however, the saturation

pulse only controls the time duration of the tag as it leaves the tagging region, and the delivery of this tag to multiple slices does not affect quantitation. Contiguous slices were acquired sequentially using gradient-recalled EPI at approximately 80-ms intervals, starting with the most proximal slice location. Using this order of slice acquisition, more distal slices that naturally have a longer transit delay δt are imaged later, and Eq. [4] is more likely to be satisfied. With this proximal-to-distal slice order, there is the possibility that acquisition of the proximal slices will interfere with tagged blood that will be delivered to more distal slices. However, for this to occur, tagged blood would have to be flowing at a velocity that is greater than the propagation velocity of the slice acquisitions. In this study, this velocity is 10 cm/s. Whereas blood in large arteries certainly travels at higher velocities, blood that is within a few centimeters of its target capillary bed is not likely to be traveling this fast. Based on measured transit times using ASL, we have estimated the average

flow velocity in the range 1–3 cm proximal to the imaging slice to be approximately 7 cm/s (data not shown). Furthermore, if blood is traveling faster than 10 cm/s, it should arrive at the imaging slice well before typical values of T_{I2} (1200–1600 ms), thus avoiding this artifact.

To determine the absolute scale of the perfusion map, both the signal from fully T_1 relaxed blood (M_{0B}) and the T_{1B} must be known. In this study, T_{1B} was assumed to be 1300 ms, and M_{0B} was estimated by imaging as follows. Because the EPI images have low spatial resolution, it was not possible to accurately measure signal from blood directly in those images. In a proton density weighted, high-resolution, gradient-echo conventional image (TE = 5 ms, TR = 1000 ms, $\alpha = 10^\circ$), the measured ratio R of proton density of blood in the sagittal sinus to that of white matter was 1.06. In a single-shot EPI image (TR = ∞), the signal M_{0wm} from white matter was measured. The fully T_1 relaxed signal from blood was then taken to be $M_{0B} = RM_{0wm}e^{(1/T_{2wm} - 1/T_{2B})TE}$, where assumed values of T_{2wm} and T_{2B} were 80 ms and 200 ms, respectively.

In calculating the signal-to-noise ratio (SNR) of the perfusion measurements, the signal is defined as the measured difference signal, and the noise is defined as the standard error of the time domain perfusion signal after pairwise subtraction, but before averaging. Rather than taking, for

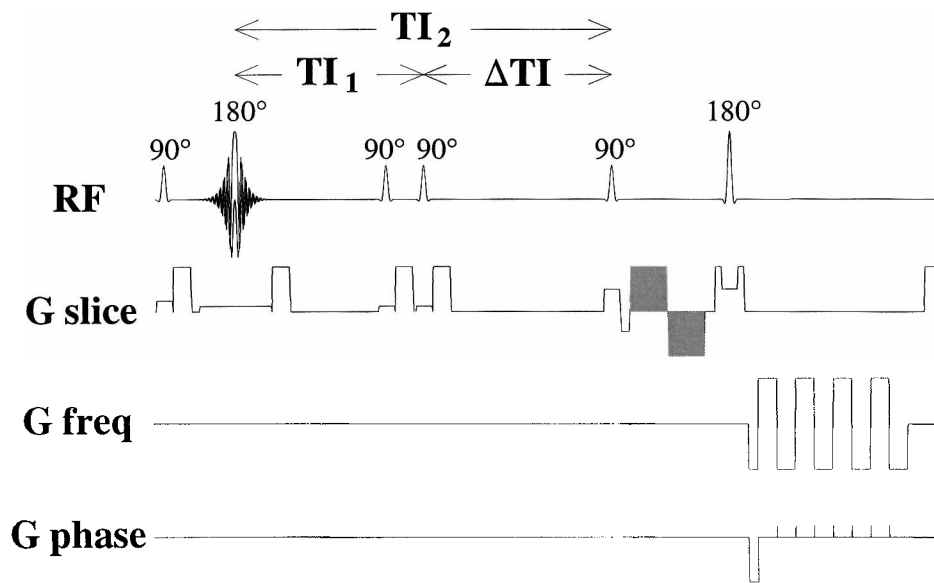


FIG. 2. Pulse sequence for QUIPSS/QUIPSS II. RF pulses (from left) are: (1) in-plane presaturation (sinc); (2) inversion tag or control (hyperbolic secant); (3–4) double saturation (two sequential sinc pulses) in imaging plane (QUIPSS) or tagging region (QUIPSS II); (5) 90° excitation pulse (sinc); (6) 180° refocusing pulse (sinc, optional). Bipolar gradient pulse shown shaded on the slice select axis is a flow/diffusion-weighting pulse that is sometimes used to dephase intravascular signal. Image acquisition is single-shot blipped EPI.

example, a region of interest (ROI) in gray matter versus an ROI outside of the head, this includes within the noise both thermal noise and physiological fluctuations, giving a realistic measure of the sensitivity of the technique.

RESULTS

Difference images for QUIPSS and QUIPSS II are shown in Fig. 3 as a function of ΔTI for QUIPSS and TI_1 for QUIPSS II, for fixed $TI_2 = 1200$ ms. The obvious qualitative difference between QUIPSS and QUIPSS II is that the QUIPSS signal seems less spatially homogeneous. This is due to the fact that QUIPSS measures tagged blood that enters the imaging slice in the period ΔTI immediately preceding image acquisition and is, therefore, relatively sensitive to artifacts from intravascular tagged blood. QUIPSS II measures a bolus of tagged blood that leaves the tagging area relatively early and has more time to distribute into smaller vessels and brain tissue.

For QUIPSS, ΔM should be proportional to ΔTI , whereas for QUIPSS II, ΔM should be proportional to TI_1 , provided that Eqs. [2] and [4] are satisfied. Plots of the average perfusion in large gray matter and

white matter ROIs versus ΔTI and TI_1 are shown in Fig. 4. The ROIs used for gray matter and white matter were derived from anatomical T_1 -weighted fast low angle shot (FLASH) images using simple intensity thresholds and are shown in Fig. 4. For the gray matter ROI, average measured perfusion values for $\{\Delta TI/TI_1\} = 600$ ms was 30.0 ± 9.1 ml/100 ml/min for QUIPSS and 65.8 ± 9.0 ml/100 ml/min for QUIPSS II. This rather large difference between QUIPSS and QUIPSS II signals is probably largely an underestimation of perfusion in QUIPSS. In QUIPSS, it is assumed that only tagged blood is entering each voxel for the entire time ΔTI (Eq. [2]). This assumption is not likely to be fulfilled for two reasons. First, because the dispersion of transit times across an imaging slice is known to be large (18, 19), it is difficult

to find a window in time ΔTI , during which tagged blood is flowing into every voxel in an imaging slice, even if flow in each vessel can be approximated by plug flow. Second, it is assumed in QUIPSS, but not QUIPSS II, that tagged blood enters the slice as a rectangular bolus, thus leading to a linear increase in difference signal over the time period. This is only true for plug flow, and in the presence of laminar or turbulent flow, the tagged bolus will be spread in time, leading to a decrease in the rate of inflow of tagged blood and an underestimation of CBF.

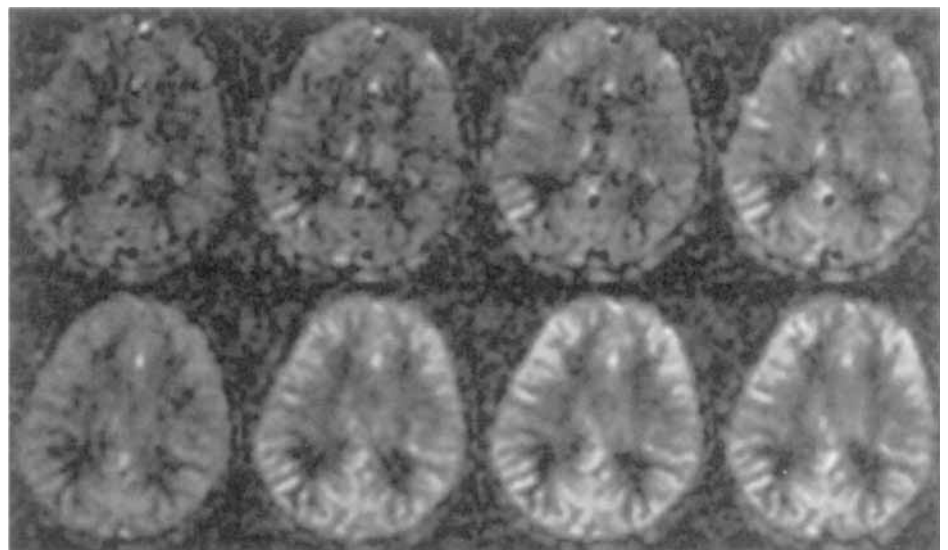


FIG. 3. Difference images (control, tag) for QUIPSS at $\Delta TI = \{200, 400, 600, 800\}$ ms (top row), and QUIPSS II at $TI_1 = \{200, 400, 600, 800\}$ ms (bottom row). TI_2 was fixed at 1200 ms for both QUIPSS and QUIPSS II.

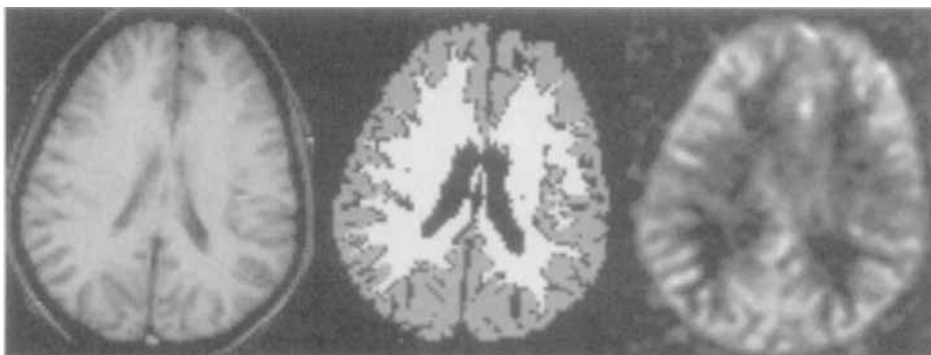
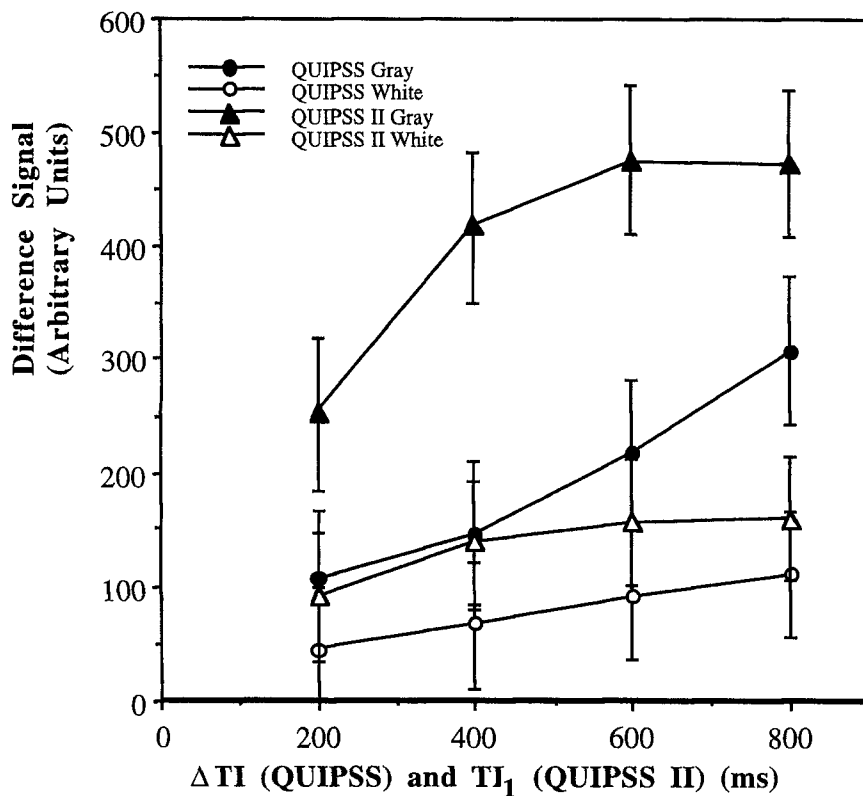


FIG. 4. Average difference signal over gray matter and white matter ROIs for images of Fig. 3. QUIPSS signal is shown versus ΔTI , and the QUIPSS II signal is shown versus TI_1 , the timing parameters to which these techniques are ideally proportional. Error bars represent noise measured as described in the text. In the image is shown a map of the gray matter and white matter ROIs used for this measurement (from left to right): the FLASH anatomical image from which the ROIs were derived by simple thresholding; gray matter ROI (shown in gray) and white matter ROI (shown in white); a representative image from the QUIPSS II series of Fig. 3.

The gray:white perfusion ratio is 2.35 for QUIPSS and 3.04 for QUIPSS II. Although these ratios are consistent with previous measurements, in our measurements, they are probably significantly lowered due to partial volume effects. The average gray matter perfusion is lowered by partial voluming with white matter, whereas the white matter perfusion is high for the same reason. In fact, for small ROIs in gray and white matter, the typical ratio is in the range 4–8, and qualitatively, it is usually difficult to discern the difference between white matter and noise (or cerebrospinal fluid). The perfusion signal that is seen

in portions of the lateral ventricles is a consistent finding and is probably choroid plexus.

Difference images from a five-slice measurement are shown in Fig. 5, along with FLASH anatomical images at the same slice locations. These difference images are not corrected for the different amounts of T_1 decay across slices that are caused by sequential image acquisition, as can be seen in the slight decrease in the difference signal with more distal slices. Note that all areas of gray matter seen in the anatomical images are represented as areas of high perfusion, whereas the perfusion in white matter areas is consistently and markedly lower.

DISCUSSION

For quantitation of perfusion, QUIPSS and QUIPSS II, in principle, eliminate the problem of the variable transit delay between the tag and the entry of blood into the slice. However, several additional effects can create systematic errors in the perfusion measurement. Probably the two largest of these effects are: the inclusion of blood that is flowing through the imaging slice in the perfusion signal; and exchange of tagged water from blood into brain tissue, changing the T_1 decay rate of the tag. There is still much work to do in the characterization of known sources of error, and it is only after these are understood that validation of the absolute numbers for CBF is useful.

The first of these effects (which we will refer to as the “flow-through” effect) is more prevalent in QUIPSS than QUIPSS II. In general, most tagged blood entering a slice is destined to perfuse tissues distal to the imaging slice. In QUIPSS II, because of the time gap ΔTI after the last tagged blood leaves the tagging region, there is time for this tagged arterial blood to flow through and exit the imaging slice before image acquisition. However, venous blood, which is generally flowing slower than arterial blood, may not have time to flow through the imaging slices, resulting in artifactual signal, as seen in the sagittal sinus and other large veins

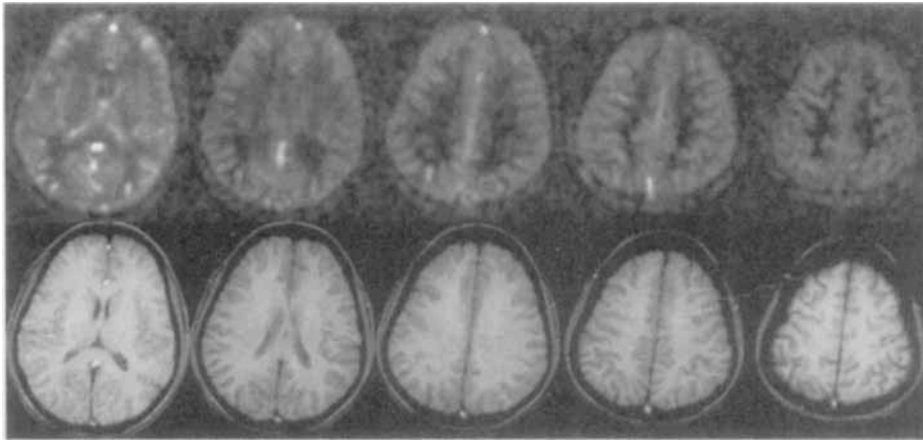


FIG. 5. Difference images from a five-slice QUIPSS II experiment, along with anatomical FLASH images from the same slices. Total imaging time was 3 min 20 s. Note that all areas of gray matter in anatomical images are represented as areas of high perfusion.

in Fig. 5. Fortunately, because venous blood is generally accelerating as it flows and arterial blood is decelerating, tagged venous blood is flowing fast at the time of image acquisition and signal from these veins can be destroyed with very small flow-weighting gradients. In QUIPSS, tagged blood is imaged immediately after the end of the bolus enters the imaging slice, and much of the tag does not have time to flow through before image acquisition, leading to artifactual focal intravascular signals from both arteries and veins. In addition, because in QUIPSS the image is acquired immediately after entry of tagged blood into the slice, there is little time for blood that travels within the imaging plane to the target capillary bed to do so, and much of the QUIPSS signal is intravascular, regardless of T_{I_2} .

When tagged blood water exchanges into brain tissue, the rate of T_1 decay of the tag shifts from that of blood to that of brain tissue. To quantify perfusion, this decay must be estimated. In Eqs. [1], [3], and [5], this decay is assumed to be at the T_1 of blood, but in fact, the exchange of tagged blood water into brain tissue occurs at a time that is comparable to typical values of T_{I_2} (1200–1600 ms). In conventional (non-QUIPSS) pulsed ASL, we find that the apparent diffusion coefficient of the perfusion signal decreased markedly at values of TI of approximately 1000 ms after the application of the tag (data not shown), and similar effects have been demonstrated by others (19). Because QUIPSS measures tagged water that recently entered the imaging slice, the QUIPSS signal is more likely to be primarily intravascular, whereas in QUIPSS II, there is more time for exchange into tissue. Thus, the approximation that the decay of the tag is at the T_1 of blood introduces less error in QUIPSS than in QUIPSS II. In summary, QUIPSS is more sensitive to the flow-through effect, whereas QUIPSS II is more sensitive to the exchange effect.

To generate quantitative perfusion maps, we are dependent on B_1 homogeneity across the slice (or knowledge of the B_1 distribution). For most birdcage type volume coils, B_1 homogeneity is very good. However, for most other coils, B_1 can vary significantly across an imaging slice. An alternative method of normalization is to

divide the perfusion signal by the magnitude of an anatomical image. If the anatomical image is cerebrospinal fluid suppressed and designed to give minimal gray-white contrast, then normalizing in this manner gives perfusion in units of volume of blood delivered per unit volume of brain tissue per unit time, independent of B_1 homogeneity.

For functional MRI, ASL techniques generally have several interesting properties. Because of the alternation between tag and control states, the perfusion signal is much less sensitive to slow subject motion than the blood oxygen

level dependent (BOLD) signal. Because the ASL signal comes primarily from small arteries and brain tissue, it is likely better localized to the site of neuronal activity than the BOLD signal (8, 25, 26). Unfortunately, the magnitude of the perfusion signal is approximately half that of the BOLD signal at 1.5 T (25). For simultaneous perfusion and BOLD imaging, pulsed ASL has the useful property that when in-plane presaturation is used, the average of temporally adjacent tag and control images gives a BOLD signal, whereas the difference between tag and control images gives the perfusion signal and the perfusion and BOLD signals are cleanly separated (8). This is due to the relationship between the relaxation curves of the inflowing blood and the static tissue. In the tag state, the tagged blood follows an inversion recovery curve ($M_z = M_{0B}(1 - 2e^{-t/T_{1B}})$), whereas in the control state, it is fully relaxed ($M_z = M_{0B}$). The difference signal between these states is proportional to flow (Eqs. [1], [3], and [5]), and independent of the static tissue signal (except for the exchange effects discussed above). However, if tag and control states are averaged, rather than subtracted, then the inflowing blood is equivalently following a saturation recovery curve ($M_{0B}(1 - 2e^{-t/T_{1B}}) + M_{0B})/2 = M_{0B}(1 - e^{-t/T_{1B}})$). With in-plane presaturation, the static tissue follows a saturation recovery curve as well; therefore, the average signal (tag + control)/2 is flow independent, again except for the relatively small effects of exchange of water between blood and tissue.

Furthermore, QUIPSS II provides a reliable way of measuring the fractional change in flow with activation directly from ASL data, without requiring measurement of a calibration factor, and without systematic errors due to changes in the δt that accompany activation. In contrast, FAIR imaging at a single TI to measure fractional flow changes with activation (27) will suffer from a systematic overestimation of the flow increase due to shortened δt with activation (15, 16).

QUIPSS II is amenable to multislice imaging, whereas QUIPSS is not. In QUIPSS, it is assumed that immediately after the saturation at T_{I_1} , tagged blood flows into the imaging slice. This condition can only be met for one slice, because the saturation of any one slice destroys

tagged magnetization that is destined to flow into more distal slices. In QUIPSS II, the saturation at T_1 only controls the bolus of tagged blood leaving the tagging region, and it is possible to allow sufficient time for this bolus to be delivered to a series of slices before image acquisition.

QUIPSS II is analogous to the most recent versions of continuous ASL in which a flow-dependent inversion tag is applied, but then halted, and a delay is inserted before image acquisition (11). Although the tagging time is typically longer, this can be viewed as a tagged bolus that is delivered to the imaging region, followed by image acquisition. In both techniques, a bolus of well-defined time width is generated by the tagging method, and a delay is introduced to allow all of the tagged blood to enter the imaging slices. Whereas under ideal circumstances the SNR of continuous ASL is greater than that of pulsed ASL by a factor of e (13, 16, 28), in practice, the difference in SNR is much smaller for four reasons. First, the delay between the generation of the tag and image acquisition decreases this difference due to relaxation of the tag. Second, the delay in continuous ASL is typically larger because the physical gap between the tag plane and the most proximal image is typically larger (8, 11, 13). Third, the inversion efficiency of pulsed ASL is generally higher than that of continuous ASL. Fourth, the optimal TR for continuous ASL is longer than that of pulsed ASL, decreasing the SNR per unit time. We are currently working on a theoretical and experimental analysis of these differences.

In conclusion, we have described two modifications of pulsed ASL that specifically address the problem of the spatially dependent transit delay between the tagging region and the imaging slice. QUIPSS has the advantage that it is relatively insensitive to the effects of water exchange into brain tissue because the signal is primarily intravascular. However, for the same reason, it is more sensitive to artifactual signal from intravascular tagged blood that is passing through the imaging slice to perfuse more distal tissues. QUIPSS II allows more time for distribution of tagged blood water into brain tissue, generating a more uniform (and presumably more accurate) gray matter perfusion signal. Also, QUIPSS II is amenable to a multislice implementation, as demonstrated here.

REFERENCES

1. P. A. Bandettini, E. C. Wong, R. S. Hinks, R. S. Tikofsky, J. S. Hyde, Time course EPI of human brain function during task activation. *Magn. Reson. Med.* **25**, 390–397 (1992).
2. S. Ogawa, D. W. Tank, R. Menon, J. M. Ellermann, S.-G. Kim, H. Merkle, K. Ugurbil, Intrinsic signal changes accompanying sensory stimulation: functional brain mapping with magnetic resonance imaging. *Proc. Natl. Acad. Sci. U. S. A.* **89**, 5951–5955 (1992).
3. K. K. Kwong, J. W. Belliveau, D. A. Chesler, I. E. Goldberg, R. M. Weisskoff, B. P. Poncelet, D. N. Kennedy, B. E. Hoppel, M. S. Cohen, R. Turner, H.-M. Cheng, T. J. Brady, B. R. Rosen, Dynamic magnetic resonance imaging of human brain activity during primary sensory stimulation. *Proc. Natl. Acad. Sci. U. S. A.* **89**, 5675–5679 (1992).
4. D. S. Williams, J. A. Detre, J. S. Leigh, A. P. Koretsky, Magnetic resonance imaging of perfusion using spin-inversion of arterial water. *Proc. Natl. Acad. Sci. U. S. A.* **89**, 212–216 (1992).
5. J. A. Detre, J. S. Leigh, D. S. Williams, A. P. Koretsky, Perfusion imaging. *Magn. Reson. Med.* **23**, 37–45 (1992).
6. R. R. Edelman, B. Siewert, D. G. Darby, V. Thangaraj, A. C. Nobre, M. M. Mesulam, S. Warach, Qualitative mapping of cerebral blood flow and functional localization with echo-planar MR imaging and signal targeting with alternating radio frequency (STAR) sequences: applications to MR angiography. *Radiology* **192**, 513–520 (1994).
7. E. C. Wong, L. R. Frank, R. B. Buxton, Quantitative multislice perfusion imaging using QUIPSS II, EPSTAR, FAIR, and PICORE, in "Proc., ISMRM, 5th Annual Meeting, Vancouver, 1997," p. 85.
8. E. C. Wong, R. B. Buxton, L. R. Frank, Implementation of quantitative perfusion imaging techniques for functional brain mapping using pulsed arterial spin labeling. *NMR Biomed.* **10**, 237–249 (1997).
9. S.-G. Kim, Quantification of regional cerebral blood flow change by flow-sensitive alternating inversion recovery (FAIR) technique: application to functional mapping. *Magn. Reson. Med.* **34**, 293–301 (1995).
10. E. C. Wong, L. R. Frank, R. B. Buxton, QUIPSS II: a method for improved quantitation of perfusion using pulsed arterial spin labeling, in "Proc., ISMRM, 5th Annual Meeting, Vancouver, 1997," p. 1761.
11. D. C. Alsop, J. A. Detre, Reduced transit-time sensitivity in noninvasive magnetic resonance imaging of human cerebral blood flow. *J. Cereb. Blood Flow Metab.* **16**, 1236–1249 (1996).
12. F. Calamante, S. R. Williams, N. V. Bruggen, K. K. Kwong, R. Turner, A model for quantification of perfusion in pulsed labelling techniques. *NMR Biomed.* **9**, 79–83 (1996).
13. K. K. Kwong, D. A. Chesler, R. M. Weisskoff, K. M. Donahue, T. L. Davis, L. Ostergaard, T. A. Campbell, B. R. Rosen, MR perfusion studies with T1-weighted echo planar imaging. *Magn. Reson. Med.* **34**, 878–887 (1995).
14. E. C. Wong, R. B. Buxton, L. R. Frank, Quantitative imaging of perfusion using a single subtraction (QUIPSS). *Neuroimage* **5** (1996).
15. R. B. Buxton, E. C. Wong, L. R. Frank, Quantitation issues in perfusion measurement with dynamic arterial spin labeling, in "Proc., ISMRM, 4th Annual Meeting, New York, 1996," p. 10.
16. R. B. Buxton, L. R. Frank, B. Siewert, S. Warach, R. R. Edelman, A quantitative model for EPSTAR perfusion imaging, in "Proc., SMR, 3rd Annual Meeting, Nice, 1995," p. 132.
17. R. B. Buxton, L. R. Frank, E. C. Wong, B. Siewert, S. Warach, R. R. Edelman, A general kinetic model for quantitative perfusion imaging with arterial spin labeling. *Magn. Reson. Med.*, in press.
18. E. C. Wong, R. B. Buxton, L. R. Frank, Quantitative perfusion imaging using EPSTAR and FAIR, in "Proc., ISMRM, 4th Annual Meeting, New York, 1996," p. 13.
19. F. Q. Ye, V. S. Matay, P. Jezzard, J. A. Frank, D. R. Weinberger, A. C. McLaughlin, Correction for vascular artifacts in cerebral blood flow values measured by using arterial spin tagging techniques. *Magn. Reson. Med.* **37**, 226–235 (1997).
20. E. C. Wong, P. A. Bandettini, J. S. Hyde, Echo-planar imaging of the human brain using a three axis local gradient coil, in "Proc., SMRM, 11th Annual Meeting, Berlin, 1992," p. 105.
21. E. C. Wong, E. Boskamp, J. S. Hyde, A volume optimized quadrature elliptical endcap birdcage brain coil, in "Proc., SMRM, 11th Annual Meeting, Berlin, 1992," p. 4015.
22. E. C. Wong, A. Jesmanowicz, J. S. Hyde, Coil optimization for MRI by conjugate gradient descent. *Magn. Reson. Med.* **21**, 39–48 (1991).
23. M. S. Silver, R. I. Joseph, D. I. Hoult, Selective spin inversion in nuclear magnetic resonance and coherent optics through an exact solution of the Bloch-Riccati equation. *Phys. Rev. A* **31**, 2753–2755 (1985).
24. L. R. Frank, E. C. Wong, R. B. Buxton, Slice profile effects in adiabatic inversion: application to multislice perfusion imaging. *Magn. Reson. Med.* **38**, 558–564 (1997).
25. R. B. Buxton, E. C. Wong, L. R. Frank, A comparison of perfusion and BOLD changes during brain activation, in "Proc., ISMRM, 5th Annual Meeting, Vancouver, 1997," p. 153.
26. P. A. Bandettini, E. C. Wong, Analysis of embedded contrast fMRI: interleaved perfusion, BOLD, and velocity nulling, in "Proc., ISMRM, 5th Annual Meeting, Vancouver, 1997," p. 156.
27. S.-G. Kim, N. V. Tsekos, Perfusion imaging by a flow-sensitive alternating inversion recovery (FAIR) technique: application to functional brain imaging. *Magn. Reson. Med.* **37**, 425–435 (1997).
28. D. A. Chesler, K. K. Kwong, An intuitive guide to the T1 based perfusion model. *Int. J. Imaging Syst. Technol.* **6**, 171–174 (1995).